INTERNATIONAL JOURNAL OF SUSTAINABLE CONSTRUCTION ENGINEERING AND TECHNOLOGY
ISSN: 2180-3242 e-ISSN: 2600-7959

IJSCET

Vol. 15 No. 2 (2024) 76-89
https://publisher.uthm.edu.my/ojs/index.php/ijscet

Fatigue Cracking Behaviour and Characteristics of Flexible Pavement Subjected to Freight Coal-Truck Loading

Dian M. Setiawan[1*]

[1] *Universitas Muhammadiyah Yogyakarta, 55183, INDONESIA*

*Corresponding Author: diansetiawanm@ft.umy.ac.id
DOI: https://doi.org/10.30880/ijscet.2024.15.02.007

Article Info

Received: 19 May 2023
Accepted: 18 December 2023
Available online: 11 March 2024

Keywords

Asphalt concrete, flexible pavement, freight truck, horizontal tensile strain

Abstract

Fatigue cracking is one of the varieties of flexible pavement distress caused by frequent traffic loads, and it is also a sign of structural collapse. Using finite element methods, numerical simulations were conducted to evaluate the strain changes that occur throughout the process of flexible pavement cracking. Several flexible pavement configurations with various thickness and different material properties of AC layer were developed, and several loading conditions in terms of the axle load, the speed, and the loading cycles of the freight truck were modelled. The numerical modelling showed that the greatest horizontal tensile strain in the 1st AC layer (surface course) is at the surface-centre of the pavement structure, which is predicted to be prone to top-down cracks. In other side, the greatest horizontal tensile strain in the 2nd AC layer (base course) is at the bottom-below of the tire tread, which is predicted to be vulnerable to bottom-up cracks. The outcomes of this study added to the knowledge gathered from previous studies, especially regarding the critical locations within the AC layer with the greatest magnitude of horizontal tensile strain and their potency to experience either the top-down cracking or bottom-up cracking, as well as related to the effect of slowing the truck speed and increasing both the truck's hauling load and loading cycles on the fatigue life of asphalt concrete layer. Future research needs to be done to evaluate the balance between both permanent deformation behaviour of the AC layer and to determine the optimum flexible pavement configurations.

1. Introduction

Indonesia, one of the world's greatest coal producers, is the top supplier of thermal coal, with a considerable proportion of low- and medium-quality coal. China and India account for the majority of thermal coal exports from Indonesia. Especially after the coal mining industry was reopened to international investment, Indonesia's production and export of coal, as well as the sales of domestic coal, increased dramatically over the previous three decades. If the present coal production rate continues, Indonesian coal reserves are estimated to last around 83 years. South Sumatera, South Kalimantan, and East Kalimantan provinces are the three major locations of Indonesian coal resources, whereas Java, Papua, and Sulawesi islands contain minor coal deposits (Setiawan, 2022a; Indonesia Investment, 2021).

The province of South Sumatera possesses around 85 percent of Indonesia's total coal reserves, or approximately 22.24 billion tons. Even if mining peaked at 50 million tons per year, South Sumatera's coal reserves would last for two centuries (Setiawan, 2022a; Sulistyorini, 2015). Unfortunately, South Sumatera's significant coal reserves are not backed by adequate transportation infrastructure. Concerns in Indonesia's coal

Int. J. of Sustainable Construction Engineering and Tech. Vol. 15 No. 2 (2024) p. 76-89

sector include the distance between the mining site and the shelter (stockpile), the disparities in the method of transportation choices, and the poor capacity of coal transport. Multiple small private enterprises employ the truck mode for delivering and distributing coal (single unit two-axle truck load). Unfortunately, the coal-carrying vehicles surpass the reasonable carrying limit (see Fig. 1). The trucks transport up to 25-30 tons of coal, when the recommended limit is 10-20 tons (Sulistyorini, 2015; Rakyat Sulsel, 2022). Therefore, transporting coal from South Sumatra to Lampung by truck causes damage to the road infrastructure as a result of overloading, as well as socially adverse impacts such as pollution, traffic congestion, and accidents.

Fig. 1 *Freight coal truck in South Sumatera, Indonesia*

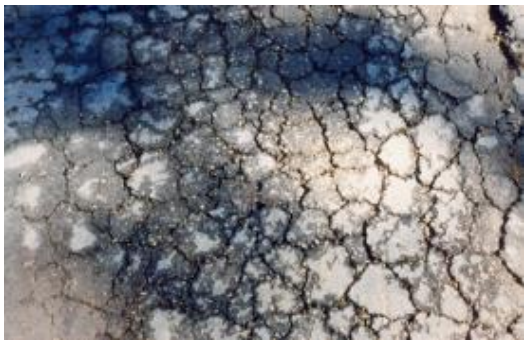

Fig. 2 *Typical alligator cracking or fatigue cracking*

Distress in the pavement is a crucial component of pavement design. The poor quality of the materials, construction, and maintenance process are the root of many problems in pavement. Pavement designers should have a better understanding of the many forms of distress since doing so would enable them to pinpoint the sources of the distress, which is crucial for maintenance and rehabilitation. Flexible pavement distresses include the following: alligator cracks (or fatigue cracks, see Fig. 2), edge cracks, potholes, longitudinal cracks, block cracks, transverse cracks, reveling/weathering (polished aggregate), rutting, bleeding, and slippage cracks (Nagy et al., 2023).

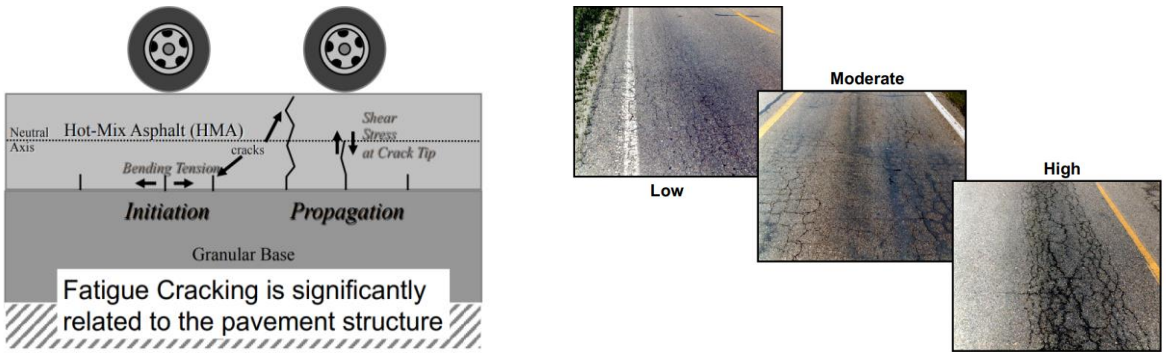

Fig. 3 *(a) Mechanism of alligator cracking or fatigue cracking; (b) severity of alligator cracking or fatigue cracking*

According to conventional wisdom, structural failure of pavements can occur in one of two ways: deformation caused by subgrade failure or fatigue cracking due to bottom-up mechanism (Hunter, 2017).

Alligator cracks or known as fatigue cracks are a load-associated structural failure (repeated tensile stress/strain at the bottom of surface layer): bottom-up cracks. Generally, begin at the wheel path and interconnected forming alligator pattern (see Fig. 3a). There are three (3) different severity level of alligator cracking or fatigue cracking, as shown in Fig. 3b. Low level: hairline fractures little wider than 1/8 inch, which may be initially linked or running parallel to one another but may also resemble an alligator pattern. Medium level: cracking producing an alligator pattern; cracks are between 1/8 and 1/4 inch wide and may be mildly spalled. High level: cracking has developed to the point that parts seem loose with badly spalled edges, cracks are likely at least 1/4 inch wide, pumping of particles through the cracks may be apparent on the surface of the pavement, and failures may be present.

Fatigue cracking is a key issue in asphalt concrete (AC) pavements because it reduces ride comfort and fuel efficiency and creates a pathway for water penetration, which causes a pavement system to degrade fast (Mensching et al., 2016). List of researchers studied this phenomenon because it significantly affects the road function and gives discomfort to the users and try to solve this problem. Due to repeat loading on asphalt pavement, accumulation of damage occurred which cause one of the primary distresses known as fatigue cracking (Asmael et al., 2020).

When the pavement has reached the end of its useful life and the asphalt binder is rigid, fatigue cracking develops. This period's asphalt binders are known as long-term aged asphalt binders. It is a load-related crack that developed as a result of constant loading. In order to create microcracks, the horizontal tensile stresses at the bottom of the pavement layer have to be greater than the pavement's tensile strength (Deef-Allah and Abdelrahman, 2021; Rahbar-Rastegar, 2017; Brown et al., 2009). The alligator or fatigue is a macrocrack that develops when these fractures spread (Deef-Allah and Abdelrahman, 2021; Brown et al., 2009; Deef-Allah and Abdelrahman, 2019).

Gibson et al. (2014) suggested that asphalt mixture becomes stiffer as recycle content increases. As many fatigue prediction models suggest, a higher dynamic modulus normally causes a shorter fatigue life. Although other model variables need to be considered for more accurate assessment, it would be fair to say that high recycle content could make asphalt material more vulnerable to fatigue cracking.

The aging of asphalt pavement generally results from a variety of sources, and as it ages, its stiffness steadily rises. As a result of the higher stiffness, moisture sensitivity is unavoidable (Yang et al., 2021; Saad et al., 2015). According to Das et al. (2015), as asphalt aged, its brittleness rose, its viscous qualities degraded with increasing stiffness, and its fatigue life reduced due to a loss of adhesion and viscosity between the aggregate and asphalt binder.

The development of fatigue cracking in cold recycled mixes under various curing durations was studied by Xia et al. (2022). Due to its benefits for ecosystems and resources, such as the high RAP utilization ratio, energy conservation, and emissions reduction, cold recycled technology has spread quickly around the world (Chang et al., 2020; Chen et al., 2019). The significant air void (8–14%) in the cold recycled mixes, however, may result in poor fatigue cracking resistance (Grilli et al., 2016).

One of the flexible pavement distress types caused mostly by frequent traffic loading is fatigue cracking. Pavement structure failure is indicated by fatigue cracking. It enables moisture infiltration and might eventually become a pothole. The emergence of fatigue cracking will hasten the degeneration of flexible pavement. For the design, analysis, and management of pavement constructions, fatigue cracking models are crucial. The literature has two different kinds of cracking models. The first kind of model is designed to forecast the length of time until failure (given a particular failure standard, such as 25% of the total area exhibiting cracking). The goal of the other kind of model is to directly forecast the cracking area as a function of a collection of factors. In order to account for numerous uncertainties, prior researchers have recommended a probabilistic technique for the first category of models called survival modeling (or duration modeling) (Gao et al., 2012).

Additionally, a variety of formulae exist that make it possible to determine how much load a pavement can support before failing. For instance, a formula to determine the critical strain in a dense bitumen macadam made with 100 pen bitumen used in the United Kingdom (UK) pavement design (Powell et al., 1984), other formulae were developed by the University of Nottingham (Brown and Brunton, 1986) and by the University of Kentucky (Setiawan, 2021; Setiawan, 2022b; Setiawan, 2022c) to determine the tensile strain at the base of the asphalt layer. However, according to Hunter (2017), these equations do not adequately describe how pavements behave. Consequently, a more mechanical approach must be used.

Using laboratory characterization and field data evaluation, several researchers have proposed predicting the performance of asphalt pavements in connection to their primary distresses. However, there is no general agreement about the laboratory testing to be carried out, the damage criterion to be taken into account, the testing condition to be set (magnitude and frequency of loading, and temperature), and the specimen geometry to be employed when studying fatigue cracking. To examine fatigue behavior and forecast fatigue life, tests in asphalt binders and mixtures are employed. The characterization of asphalt binders is important since fatigue cracking is greatly influenced by these materials' rheological properties (Bessa, 2017). However, there are limited studies that develop a finite element modeling of flexible pavement with various configurations and

different loading systems in terms of hauling loads and speed of heavy freight truck to predict the fatigue cracking performance of flexible pavements.

The issue of pavement fatigue fractures is complicated. There are no issues with calculating deformations in the lowest portion of asphalt layers since multilayer systems make this possible. However, it is important to detect the greatest horizontal tensile strain location in the interfaces part. In the present research, the linear elastic and linear viscoelastic characterization of asphalt materials were considered. In respect to the numerical modeling of flexible pavement structures, four different configurations of flexible pavement were developed. Horizontal tensile strain at the bottom of AC layer were collected. The flexible pavement models were composed by three different main layers, which are asphalt concrete, sub-base, and subgrade. Two variances of AC structures were utilized in the models based on two types of asphalt binders. The mechanical performance of each flexible pavement configurations was compared based on the magnitudes of the horizontal tensile strain as the potential indicator of the occurrence of fatigue cracking in flexible pavements.

2. Materials and Methods

2.1 Flexible Pavement Structural Configuration

Four (4) configurations of flexible pavement with the width of 3000 mm were developed and considered in this study (see Fig. 4). As shown in Fig. 4a, the first (1st) configuration consists of AC type 1 as surface layer (100 mm), AC type 2 as base layer (200 mm), followed by sub-base (400 mm) and subgrade layer (800 mm). Second (2nd) configuration, illustrated in Fig. 4b, includes the AC type 2 as surface layer (100 mm), AC type 1 as base layer (200 mm), followed by sub-base (400 mm) and subgrade layer (800 mm). Third (3rd) configuration comprise of AC type 1 (300 mm), sub-base (400 mm), and subgrade layer (800 mm), presented in Fig. 4c. Finally, Fig. 4d depicted fourth (4th) configuration, constructed with AC type 2 (300 mm), sub-base (400 mm), and subgrade layer (800 mm).

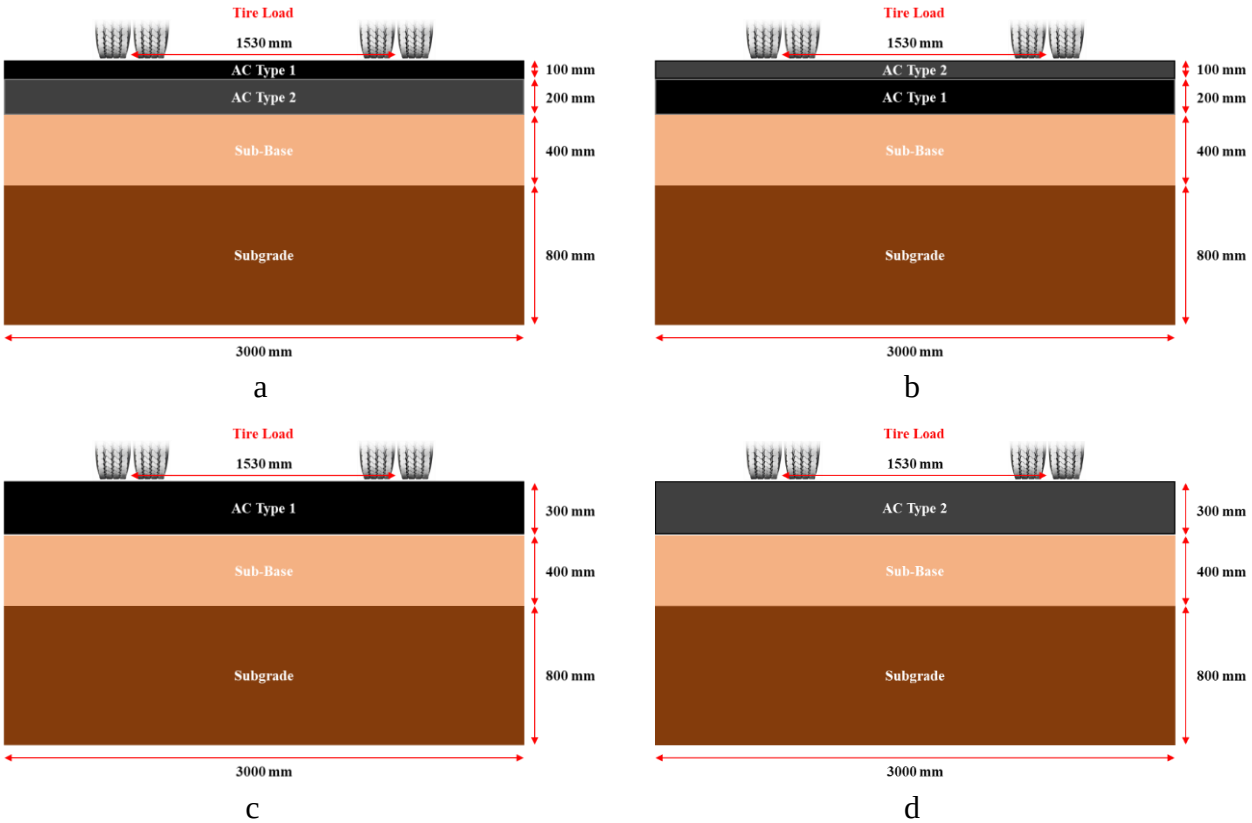

Fig. 4 *Four different flexible pavement structural configurations (a) 1st configuration; (b) 2nd configuration; (c) 3rd configuration; (d) 4th configuration*

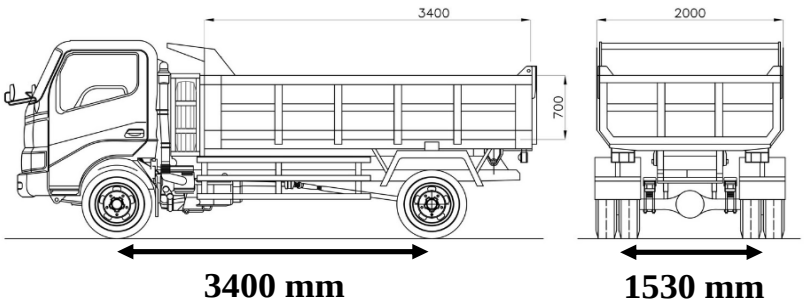

Fig. 5 *Single unit two-axle truck load*

2.2 Loading System From Freight Truck

The wheel configuration based on a single unit two-axle truck load was applied to the interior of the flexible pavement, as shown in Fig. 5. The variations of loading systems from freight trucks were based on three different running speeds (40, 60, and 80 kph), three different axle loads (5000, 12,500, and 18,000 kg), and two different loading cycles (5000 and 10,000 loading cycles). Therefore, in total there were 9 model variations (see Table 1).

Table 1 *Combination of freight truck speed, axle load, and loading cycles*

Case	Speed (km/h)	Axle Load (Kg)	Loading Cycles	Truck's Load (Kg/Truck)	Number of Truck	Hauling Capacity (Tons)
1	40					
2	60	5,000	5000	10,000	5000	50,000
3	80					
4	40					
5	60	12,500	10,000	25,000	10,000	250,000
6	80					
7	40					
8	60	18,000	10,000	36,000	10,000	360,000
9	80					

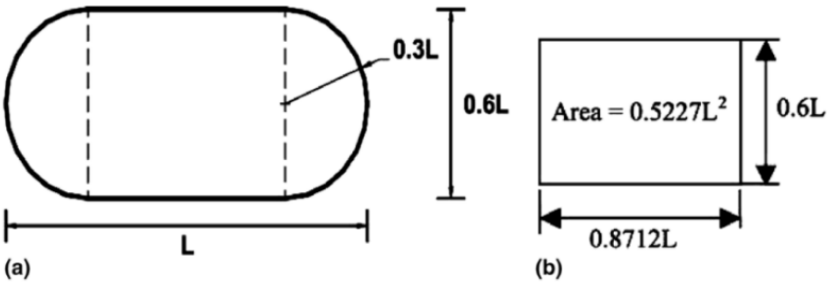

Fig. 6 *(a) Contact area between tires and the pavement surface; (b) Equivalent contact area (Setiawan, 2020; Mulungye et al., 2007; Huang, 2004)*

Fig. 6 presents the contact area between tires and the pavement surface and its equivalent contact area. As shown in Fig. 6, the freight truck load was in the form of cyclic pressure load, and 1 loading cycles equal to 1 passing truck. Since L is 389 mm, one (1) wheel has the rectangular area conversion of 0.5227 L2, with a length of 0.338 m and a width of 0.234 m (Setiawan, 2020; Mulungye et al., 2007; Huang, 2004).

2.3 Material Properties

The material properties of AC type 1 and AC type 2 were obtained from Lee et al. (2018), considering the linear elastic and viscoelastic characteristics. The material properties of sub-base granular and soil subgrade layer are typical values used in Indonesian Standard and Regulation. Table 2 presents the elastic parameters of the

Int. J. of Sustainable Construction Engineering and Tech. Vol. 15 No. 2 (2024) p. 76-89

materials considered in this study. The Prony series for linear viscoelastic properties of asphalt can be found in Lee et al. (2018).

Table 2 *Material properties of asphalt concrete, sub-base granular, and soil subgrade layer*

Structural Layer	Mass Density (Kg/m³)	Elastic Modulus, E (GPa)	Poisson's Ratio
AC Type 1 (Lee et al., 2018)	2345.35	25,2	0.35
AC Type 2 (Lee et al., 2018)	2345.35	22,9	0.35
Sub-Base	1900	0.12	0.30
Subgrade	2000	0.06	0.25

2.4 Construction of the Model

Fig. 7 depicts the flexible pavement structural configurations in 2-dimensional model using ABAQUS software. The interaction of each layer is considered as glued, to simplify the model. Element CPE3, 3-node linear plane strain triangle, was selected for the 1st AC layer (structured), and 2nd AC layer (free). In addition, element CPE4, 4-node bilinear plane strain quadrilateral, was appointed for sub-base (structured) and subgrade (structured).

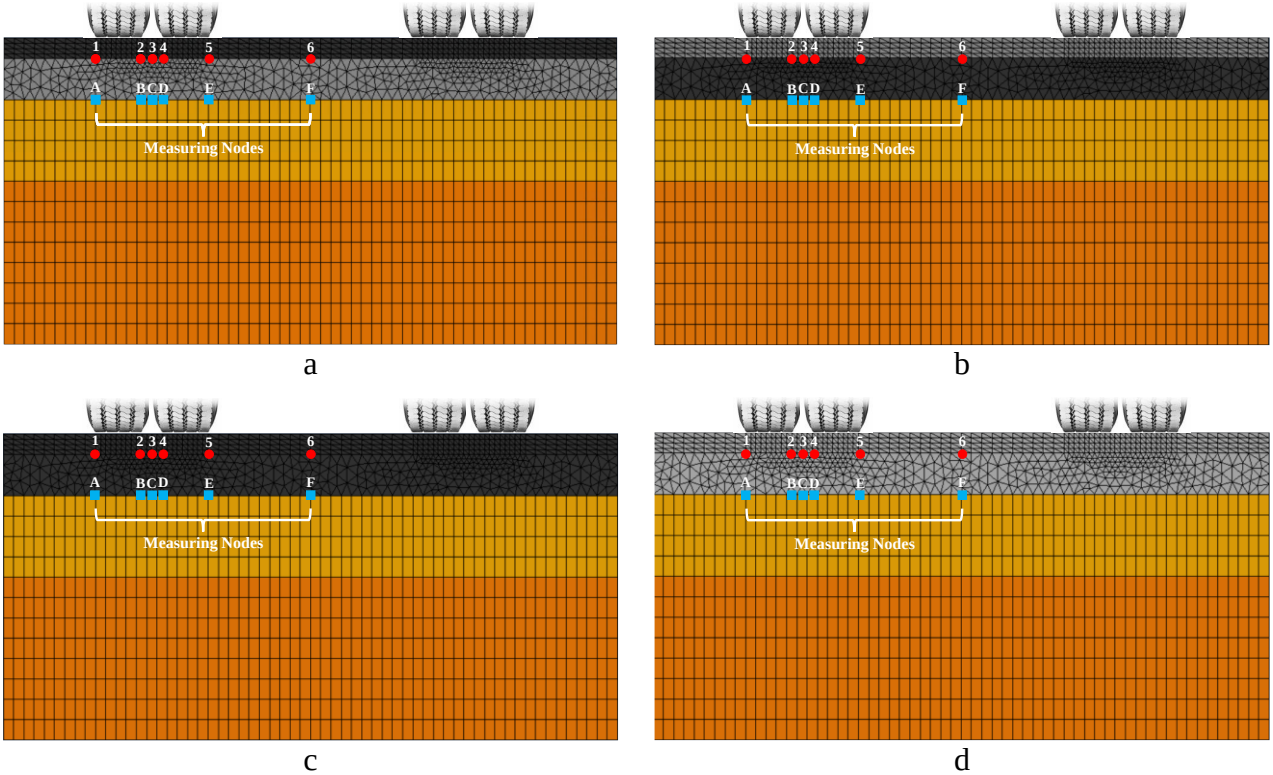

Fig. 7 *Flexible pavement in 2-dimensional model and measuring nodes (a) 1st configuration; (b) 2nd configuration; (c) 3rd configuration; (d) 4th configuration*

The mesh size of 0.025 m x 0.025 m was created below tire footprints, followed by 0.025 m x 0.05 for the 1st AC layer, 0.05 m x 0.05 m for the 2nd AC layer, and 0.05 m x 0.1 m for both the sub-base and subgrade layer. Furthermore, the red dots and blue dots in Fig. 7 are the location of measuring nodes to obtain the magnitude of horizontal tensile strain at the bottom of the 1st AC layer (nodes 1, 2, 3, 4, 5, and 6) and 2nd AC layer (nodes A, B, C, D, E, and F), respectively.

3. Results

3.1 Horizontal Tensile Strains in Critical Locations

The standard convention in this study is that compressive strains are negative and tensile strains are positive. In other words, a positive strain value corresponds to a tensile, while negative strain value corresponds to a compressive.

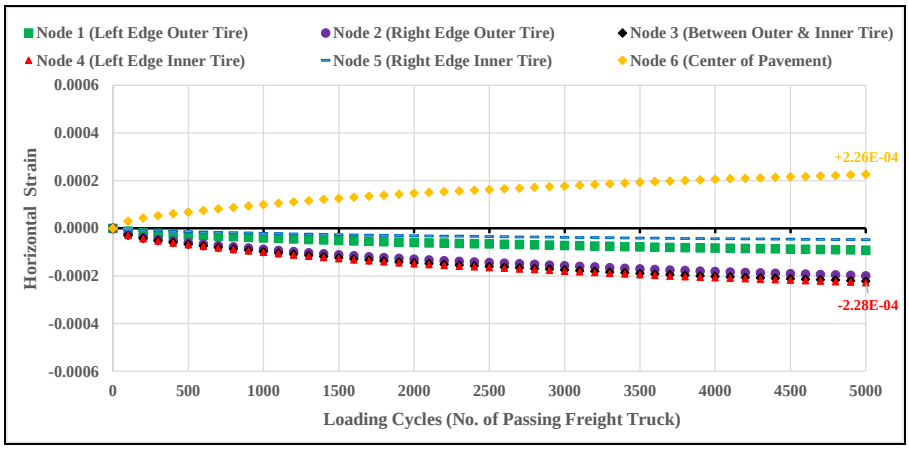

Fig. 8 *Horizontal tensile strains at six (6) different locations of measuring nodes at the bottom of the 1st AC layer (nodes 1, 2, 3, 4, 5, and 6 in AC type 1) in flexible pavement 1st configuration and 1st case (10 tons/truck, 40 kph, 5000 loading cycles)*

In the first stage of the analysis in this study, the horizontal tensile strains at six (6) different locations of measuring nodes at the bottom of the 1st AC layer (nodes 1, 2, 3, 4, 5, and 6 in AC type 1) in flexible pavement 1st configuration and 1st case (see Fig. 7a) were measured to obtain the critical location with the greatest horizontal tensile strain magnitude. As illustrated in Fig. 8, the greatest compressive strain (negative strain) in the 1st AC layer (AC type 1) of flexible pavement 1st configuration and 1st case is at measuring node 4 (below the left edge of inner tire, see Fig. 7a), followed by compressive strain at measuring node 3 (between outer and inner tire, see Fig. 7a), then at measuring node 2 (below the right edge of outer tire, see Fig. 7a), at measuring node 1 (below the left edge of outer tire, see Fig. 7a), and finally the compressive strain at measuring node 5 (below the right edge of inner tire, see Fig. 7a). In other side, the greatest horizontal tensile strain (positive strain) in the 1st AC layer (AC type 1) of flexible pavement 1st configuration and 1st case is at measuring node 6 (below the center of the pavement structure, see Fig. 7a).

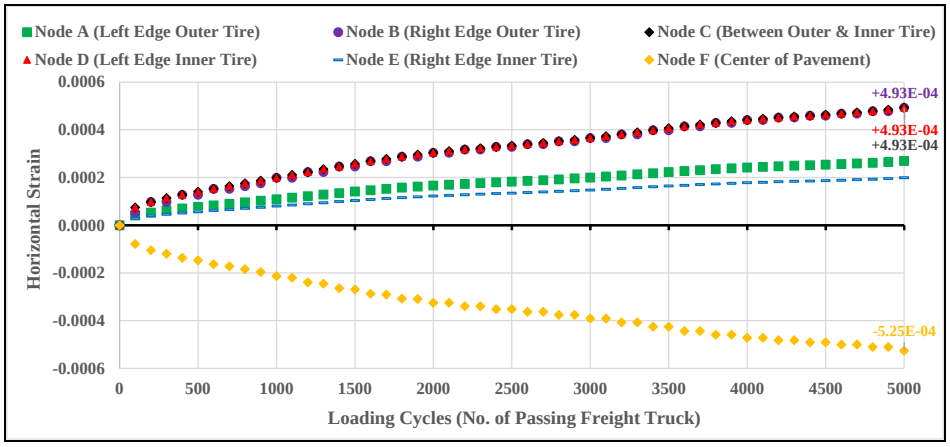

Fig. 9 *Horizontal tensile strains at six (6) different locations of measuring nodes at the bottom of the 2nd AC layer (nodes a, b, c, d, e, and f in AC type 2) in flexible pavement 1st configuration and 1st case (10 tons/truck, 40 kph, 5000 loading cycles)*

In the second stage, the horizontal tensile strains at six (6) different locations of measuring nodes at the bottom of the 2nd AC layer (nodes A, B, C, D, E, and F in AC type 2) in flexible pavement 1st configuration and 1st case (see Fig. 7a) were computed in order to obtain the critical location with the greatest horizontal tensile strain magnitude. As illustrated in Fig. 9, the greatest compressive strain (negative strain) in the 2nd AC layer (AC type 2) of flexible pavement 1st configuration and 1st case is at measuring node F (below the center of the pavement structure, see Fig. 7a). In other side, the magnitude of the horizontal tensile strain (positive strain) at measuring node B (below the right edge of outer tire, see Fig. 7a), at measuring node C (between outer and inner tire, see Fig. 7a), and measuring node D (below the left edge of inner tire, see Fig. 7a) are similar. Also, those

Int. J. of Sustainable Construction Engineering and Tech. Vol. 15 No. 2 (2024) p. 76-89

three locations are known as the critical locations with the greatest horizontal tensile strain (positive strain) in the 2nd AC layer (AC type 2) of flexible pavement 1st configuration and 1st case, followed by the horizontal tensile strain at measuring node A (below the left edge of outer tire, see Fig. 7a), and horizontal tensile strain at measuring node E (below the right edge of inner tire, see Fig. 7a).

3.2 Effect of Freight Truck Loads, Speed, and Loading Cycles on Horizontal Tensile Strains

In order to analyze the effect of various freight truck hauling loads, speed, and loading cycles on the flexible pavement (1st configuration) mechanical behavior in terms of the potential of fatigue cracking in AC layer, therefore Fig. 10 and Fig. 11 present the results of 9 cases that have been modeled in ABAQUS software. The details of each case can be found in Table 2. It can be seen that, within the same magnitude of truck's hauling load and the same number of passing trucks (case 1 vs. case 2 vs. case 3; case 4 vs. case 5 vs. case 6; and case 7 vs. case 8 vs. case 9), the lower the truck speed, the greater the horizontal tensile strain at the bottom of the 1st AC layer (see Fig. 10) and 2nd AC layer (see Fig. 11), respectively.

As depicted in Fig. 10, within the same magnitude of truck's hauling loads, 10 tons or 25 tons or 36 tons, and the same number of passing trucks, 5000 or 10,000, decreasing the truck speed 25% lower, from 80 to 60 kph (case 3 vs. case 2 or case 6 vs. case 5 or case 9 vs. case 8), will increase the magnitude of horizontal tensile strain at the bottom of the 1st AC layer approximately 5%. Moreover, within the same magnitude of truck's hauling loads, 10 tons or 25 tons or 36 tons, and the same number of passing trucks, 5000 or 10,000, decreasing the truck speed 33% lower, from 60 to 40 kph (case 2 vs. case 1 or case 5 vs. case 4 or case 8 vs case 7), will increase the magnitude of horizontal tensile strain at the bottom of the 1st AC layer about 10%.

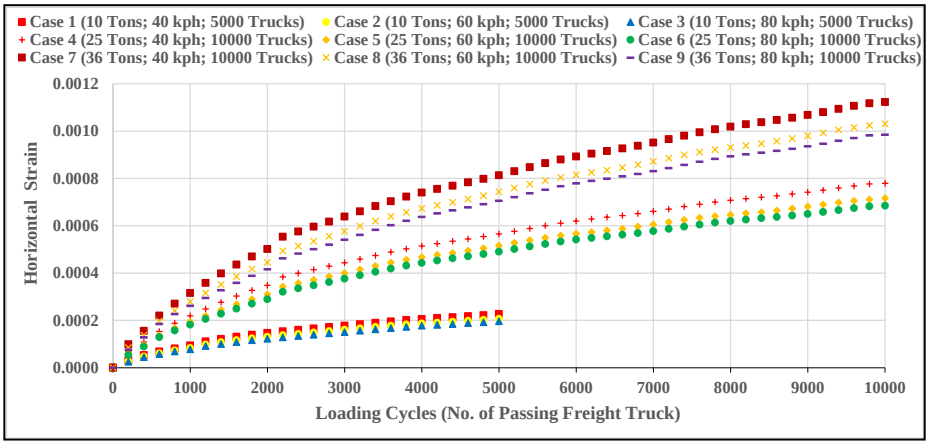

Fig. 10 *The greatest horizontal tensile strain at the bottom of the 1st AC layer (nodes 6 in AC type 1) in flexible pavement 1st configuration for various magnitudes and combination of freight truck loads, speeds, and loading cycles*

Fig. 10 also shown that, within the same magnitude of truck speed, 40 kph or 60 kph or 80 kph, increasing the truck's hauling loads 1.5 times greater, from 10 to 25 tons, and the number of passing trucks 1 times higher, from 5000 to 10,000 (case 1 vs case 4 or case 2 vs. case 5 or case 3 vs case 6) will increase the magnitude of horizontal tensile strain at the bottom of the 1st AC layer around 2.5 times. In other words, increasing the hauling capacity 5 times, from 50,000 tons to 250,000 tons, will increase the risk of fatigue cracking in the 1st AC layer by 2.5 times. Furthermore, within the same magnitude of truck speed, 40 kph or 60 kph or 80 kph, and the same number of passing trucks, 10,000, increasing the truck loads 44% from 25 to 36 tons (case 4 vs. case 7 or case 5 vs. case 8 or case 6 vs case 9) will increase the magnitude of horizontal tensile strain at the bottom of the 1st AC layer also about 44%. In other words, increasing the hauling capacity by 44%, from 250,000 tons to 360,000 tons, will also increase the risk of fatigue cracking in the 1st AC layer by 44%.

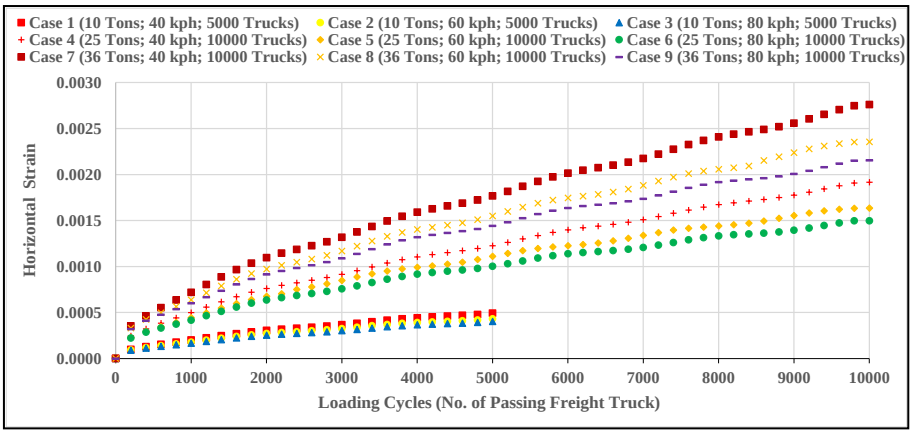

Fig. 11 *The greatest horizontal tensile strain at the bottom of the 2nd AC layer (nodes b, c, or d in AC type 2) in flexible pavement 1st configuration for various magnitudes and combination of freight truck loads, speeds, and loading cycles*

As described in Fig. 11, within the same magnitude of truck's hauling loads, 10 tons or 25 tons or 36 tons, and the same number of passing trucks, 5000 or 10,000, decreasing the truck speed 25% lower, from 80 to 60 kph (case 3 vs. case 2 or case 6 vs. case 5 or case 9 vs. case 8), will increase the magnitude of horizontal tensile strain at the bottom of the 2nd AC layer approximately 7-9%. Moreover, within the same magnitude of truck's hauling loads, 10 tons or 25 tons or 36 tons, and the same number of passing trucks, 5000 or 10,000, decreasing the truck speed 33% lower, from 60 to 40 kph (case 2 vs. case 1 or case 5 vs. case 4 or case 8 vs case 7), will increase the magnitude of horizontal tensile strain at the bottom of the 2nd AC layer about 14-17%.

Fig. 11 also represented that, within the same magnitude of truck speed, 40 kph or 60 kph or 80 kph, increasing the truck' hauling loads 1.5 times greater, from 10 to 25 tons, and the number of passing trucks 1 times higher, from 5000 to 10,000 (case 1 vs case 4 or case 2 vs. case 5 or case 3 vs case 6) will increase the magnitude of horizontal tensile strain at the bottom of the 2nd AC layer around 2.7-2.9 times. In other words, increasing the hauling capacity 5 times, from 50,000 tons to 250,000 tons, will increase the risk of fatigue cracking in the 2nd AC layer by 2.7-2.9 times. Furthermore, within the same magnitude of truck speed, 40 kph or 60 kph or 80 kph, and the same number of passing trucks, 10,000, increasing the truck loads 44% from 25 to 36 tons (case 4 vs. case 7 or case 5 vs. case 8 or case 6 vs case 9) will increase the magnitude of horizontal tensile strain at the bottom of the 2nd AC layer also about 44%. In other words, increasing the hauling capacity by 44%, from 250,000 tons to 360,000 tons, will also increase the risk of fatigue cracking in the 1st AC layer by 44%.

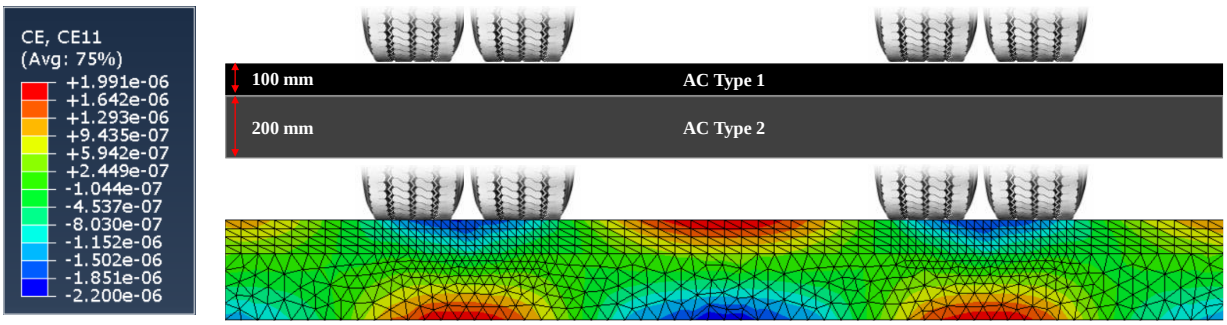

Fig. 12 *Strain distribution within AC layer structure in flexible pavement 1st configuration*

Int. J. of Sustainable Construction Engineering and Tech. Vol. 15 No. 2 (2024) p. 76-89

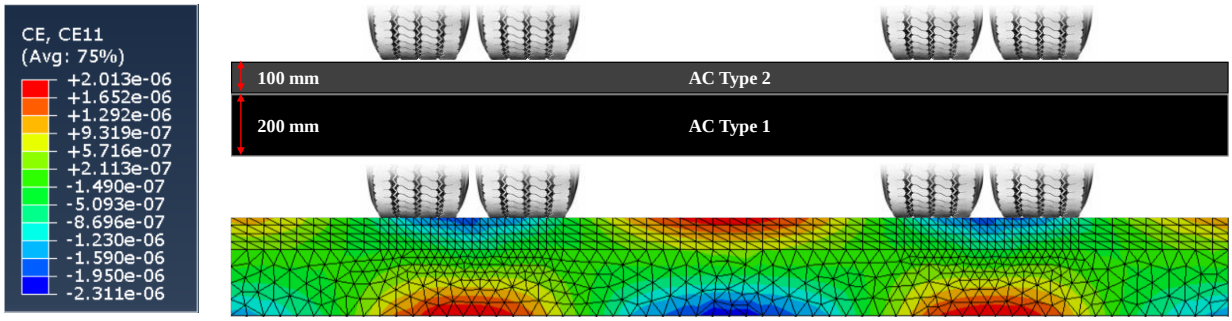

Fig. 13 *Strain distribution within AC layer structure in flexible pavement 2nd configuration*

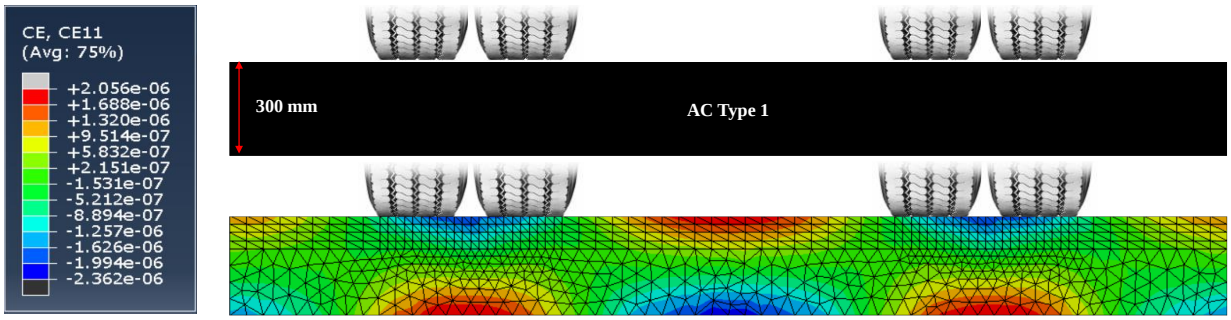

Fig. 14 *Strain distribution within AC layer structure in flexible pavement 3rd configuration*

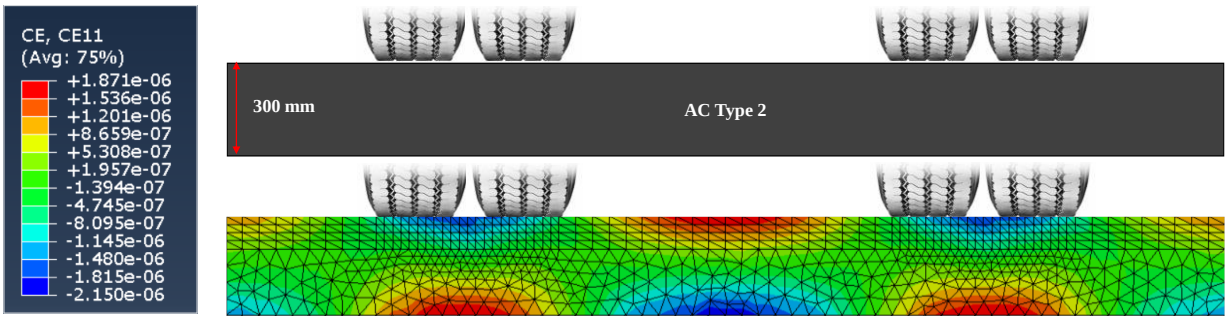

Fig. 15 *Strain distribution within AC layer structure in flexible pavement 4th configuration*

3.3 Horizontal Tensile Strains in Various Configurations of Flexible Pavement

In order to obtain the optimum design of flexible pavement with minimum horizontal tensile strain at the bottom of the AC layer, this study proposed four (4) different configurations of flexible pavement based on two (2) types of AC structures utilization, AC type 1 and AC type 2, as well as three level of AC layer thicknesses, 100 mm, 200 mm, and 300 mm. In the 1st configuration, there was AC type 1 acted as AC surface layer with the thickness of 100 mm, and AC type 2 served as AC base layer with the thickness of 200 mm, so the total thickness was 300 mm (see Fig. 12). In the 2nd configuration, there were AC type 2 acted as AC surface layer with the thickness of 100 mm, and AC type 1 served as AC base layer with the thickness of 200 mm, therefore the total thickness was also 300 mm (see Fig. 13). In other side, there was only 1 (one) type of AC layer in 3rd and 4th configurations. AC type 1 with the thickness of 300 mm was utilized in 3rd configuration (see Fig. 14), while AC type 2 also with the thickness of 300 mm, was used in the 4th configuration (see Fig. 15).

Since the effect of slowing the truck speed and increasing both the truck's hauling load and loading cycles is more significant to the development of horizontal tensile strain at the bottom of the 2nd AC layer than at the bottom of the 1st AC layer. Therefore, the following stage will discuss about the effect of slowing the truck speed (case 7 vs. case 8 vs. case 9, see Fig. 16) as well as the effect of increasing both the truck's hauling load and the number of passing trucks on the magnitude of the horizontal tensile strain at the bottom of the total AC layer for the four (4) flexible pavement configurations.

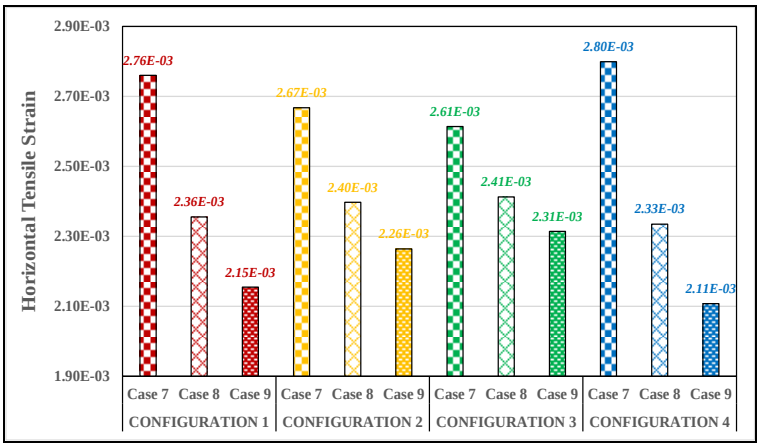

Fig. 16 *The greatest horizontal tensile strain at the bottom of AC layer in flexible pavement configuration 1, 2, 3, and 4 due to various truck speed*

4. Discussion

Anywhere a tensile tension is present within the flexible pavement, a fracture can form. The bottom part of the asphalt layers beneath the load, the surface at the edges of the load zone, and the surface in the contact region of the tire tread are three such zones that may be recognized, according to Brown (1996). The tire's edge and the surface where shear takes place are other important areas. Classical fatigue cracks are often referred to as "bottom-up" cracks. These cracks are simple to originate on the bottom of thin asphalt layers and spread upward. The bottom of the layers' poor tensile strength and concentration of recurrent tensile strains are the root causes of these problems. Another form of surface cracking mostly affects the edges of the load zone. Field testing reveal that the "top-down" crack range only extends a short distance under the surface. They often only go below 50 to 75 mm (Mackiewicz, 2018). Additionally, Mackiewicz (2018) discovered that thinner pavements are more prone to fatigue cracks that form "top-down" mechanism whereas thicker pavements are more prone to fatigue cracks that form "bottom-up" mechanism.

According to Cho et al. (2017), an asphalt pavement generally consists of one or more AC layers over underlying granular materials with a certain level of adhesion between the layers. Poor bonding between the surface layers can substantially impair the ride quality of an asphalt pavement by reducing its serviceability (Tschegg et al., 1995). Using a computational analysis software called FlexPAVETM, Cho et al. (2019) studied the impact of debonded pavement constructions on fatigue cracking performance. To ascertain the distribution of stresses and strains at the surface and interface of asphalt layers and to assess the fatigue cracking performance of debonded pavement constructions, pavement response analysis and pavement performance analysis were both carried out. They discovered that compared to a completely bonded example, a debonded pavement construction might produce much greater tensile stress levels, which would subsequently result in worse fatigue cracking performance. Additionally, the debonded surface layers of an asphalt pavement may shorten the pavement structure's ability to withstand fatigue by around 90%.

As shown in Fig. 12-15, the blue contour at the surface of AC layer (below tire tread) and at the bottom-middle of AC layer will experience the greatest compressive (negative) strains, while the red contour at the bottom of the AC layer (below tire tread) and at the surface-center of AC layer will experience the greatest horizontal tensile (positive) strains. In other words, the blue contour at the surface of AC layer (below tire tread) and at the bottom-middle of AC layer will prone to the rutting damage, while the red contour at the bottom of the AC layer (below tire tread) and at the surface-center of AC layer will prone to the fatigue cracking. Furthermore, it is predicted that the area that covered by red contour at the bottom of the AC layer (below tire tread) will suffer the bottom-up cracking process, while the area that covered by red contour at the surface-center of AC layer will suffer the top-down cracking process.

Fracture mechanics and material technology are both involved in the problem of fatigue cracking of AC. The amount of fatigue and bending experienced by the pavement's upper layers varies according to thickness (Mackiewicz, 2018; McGennis et al., 1994; Roberts et al., 1996). Fatigue degradation is more likely to affect the asphalt base than permanent deformations. Besides, the asphalt base binder course is not only vulnerable to permanent deformation, but it is also susceptible to low-temperature damage. When there is insufficient interlayer bonding between the asphalt layers, fatigue cracks are more likely to start in this layer, leading to the crack's spread to the base. In the event of loss of adhesion or the beginning of propagation from the lower layers, the surface course is vulnerable to damage from the bottom. Due to its upper position, it is also clearly

susceptible to "top-down" cracks (Mackiewicz, 2018; Jaskula, 2014; Kim et al., 2011; Mohammad et al., 2010; Wang and Al-Qadi, 2010).

As presented in Fig. 16, 3rd configuration produced the lowest horizontal tensile strain when the 10,000 trucks carrying the loads 36,000 tons/truck and passing with the speed of 40 kph, while 4th configuration has the lowest horizontal tensile strain when the 10,000 trucks also carrying the loads 36,000 tons/truck but passing with the speed of 60 and 80 kph, respectively. Also, even though the 3rd configuration has the lowest horizontal tensile strain due to the truck speed of 40 kph, however its reductions due to the increase of truck speed to 60 kph and 80 kph are only 7.7% and 4.1%. In other side, although the 4th configuration has the greatest horizontal tensile strain due to the truck speed of 40 kph, however its reductions due to the increase of truck speed to 60 kph and 80 kph are the most significant, 16.6% and 9.8%. These two conditions are possible because the AC type 2 with the thickness of 300 mm in the flexible pavement 4th configuration is softer than the AC type 1 with the same thickness, 300 mm, in the flexible pavement 3rd configuration. This can be confirmed since the elastic modulus of AC type 1 is higher than the elastic modulus of AC type 2 (see Table 2). In other words, the stiffer the AC layer and the higher the truck speed, the more prone the AC layer to the fatigue cracking.

Gibson et al. (2014) also concluded that a higher dynamic modulus normally causes a shorter fatigue life. Deef-Allah and Abdelrahman 2021) employed binders extracted and recovered (E&R) from field mixes comprising various percentages of recycled materials (reclaimed asphalt pavement (RAP) and recycled asphalt shingles (RAS)) and the performance grades of the binders. Using the Superpave fatigue cracking criteria and the number of load repetitions before failure, the fatigue resistance of the E&R binders was determined. They discovered that asphalt binders E&R from mixes with the youngest asphalt binder and the softest asphalt binder (the lowest PG temperature) exhibited the greatest resistance to fatigue cracking. Increasing the proportion of recycled materials in asphalt mixtures reduced the fatigue cracking resistance of the E&R binders.

5. Conclusions

This research was conducted to investigate the fatigue cracking behavior and characteristics of flexible pavement. The linear elastic and linear viscoelastic characterization of asphalt materials were considered in this study. Four (4) configurations of flexible pavement based on the variations in AC materials and thickness, as well as nine (9) cases of the parametric studies based on the variations in the truck's speed, hauling loads, and loading cycles, have been created in 2-dimensional model using ABAQUS software to perform the sensitivity analysis. Several critical locations within AC structures were measured to obtain the greatest horizontal tensile strain as the indicator of the occurrence of fatigue cracking in flexible pavements. The outcomes of this study added to the knowledge gathered from the previous studies. The following conclusions were taken from the analyses:

1. The greatest horizontal tensile strain in the 1st AC layer is at the surface-center of the pavement structure.
2. The magnitude of the horizontal tensile strain at below the right edge of outer tire, between outer and inner tire, and below the left edge of inner tire are similar. Those three locations are known as the critical locations with the greatest horizontal tensile strain in the 2nd AC layer.
3. Slowing the truck speed and increasing both the truck load and the number of passing trucks will enhance the magnitude of horizontal tensile strain and so that the potential of fatigue cracking occurrence. The effect of slowing the truck speed and increasing both the truck load and loading cycles is more significant to the development of horizontal tensile strain at the bottom of the 2nd AC layer than at the bottom of the 1st AC layer.
4. Furthermore, there was a proportional increase in the horizontal tensile strain at the bottom of the 1st and 2nd AC layer due to the increase of the truck's hauling loads alone or the decrease of truck speeds alone. However, there was an exponential increase in the horizontal tensile strain at the bottom of the 1st and 2nd AC layer due to the increase of both the truck's hauling loads and the number of passing trucks.
5. The surface-center area of the 1st AC layer (surface course) is vulnerable to top-down cracks, while the bottom of the 2nd AC layer (base course) is vulnerable to bottom-up cracks.

It can be suggested that the flexible pavement 2nd and 3rd configuration should be constructed to serve the operation of freight truck with the operating speed of 40 kph. In addition, the flexible pavement 1st and 4th configuration should be considered to serve the operation of freight truck with the higher operating speed, for example 60 and 80 kph. Future research needs to be done in evaluating both permanent deformation and fatigue cracking of the AC layer and to determine the optimum flexible pavement configurations.

Acknowledgement

The author would like to express gratitude to the Institute of Research, Publications & Community Service of Universitas Muhammadiyah Yogyakarta (LPPM UMY) for the Funding of Domestic Partnership Scheme 2022 (No: 20/RIS-LRI/II/2022).

References

Asmael, N. M., Fattah, M. Y. & Kadhim, A. J. (2020). Exploring the effect of warm additives on fatigue cracking of asphalt mixtures. *Journal of Applied Science and Engineering, 23*(2), pp. 197-205. DOI: http://dx.doi.org/10.6180/jase.202006_23(2).0003

Bessa, I. S. (2017). *Laboratory and Field Study of Fatigue Cracking Prediction in Asphalt Pavements*. Escola Politécnica da Universidade de São Paulo: Ph.D. Thesis.

Brown, R. B., Kandhal, P. S., Roberts, F. L., Kim, Y. R., Lee, D. Y. & Kennedy, T. W. (2009). *Hot mix asphalt materials, mixture design, and construction*. 3rd ed. NAPA Research and Education Foundation, Lanham: Maryland, USA.

Brown, S. F. & Brunton, J. M. (1986). *An introduction to the analytical design of bituminous pavements*. 3rd ed. University of Nottingham: Nottingham, UK.

Brown, S. F. (1996). Soil mechanics in pavement engineering. *Geotechnique, 46*, pp. 381-426.

Chang, X. W., Zhang, R. H., Xiao, Y., Chen. X. Y., Zhang, X. S. & Liu, G. (2020). Mapping of publications on asphalt pavement and bitumen materials: A bibliometric review. *Construction and Building Materials, 234*, 117370. DOI: https://doi.org/10.1016/j.conbuildmat.2019.117370

Chen, S. H., Zheng, W. Y. & Paramitha, P. A. (2019). Evaluation of innovative cold mix recycled asphalt concrete as backfill material in pipeline maintenance. *Journal of Testing and Evaluation, 47*(3), pp. 1864-1875. DOI: https://doi.org/10.1520/JTE20170773

Cho, S. H., Karshenas, A., Tayebali, A. A., Guddati, M. N. & Kim, Y. R. (2017). A mechanistic approach to evaluate the potential of the debonding distress in asphalt pavements. *Inter. J. Pave. Eng, 18*(12), pp. 1098-1110.

Cho, S. H., Lee, K., Mahboub, K. C., Jeon, J. & Kim, Y. R. Evaluation of fatigue cracking performance in a debonded asphalt pavement. *International Journal of Pavement Research and Technology, 12*, pp. 388-395. DOI: https://doi.org/10.1007/s42947-019-0046-8

Das, P. K., Birgisson, B., Jelagin, D. & Kringos, N. (2015). Investigation of the asphalt mixture morphology influence on its ageing susceptibility. *Materials and Structures, 48*, pp. 987-1000. DOI: https://doi.org/10.1617/s11527-013-0209-z

Deef-Allah, E. & Abdelrahman, M. (2019). Balancing the performance of asphalt binder modified by tire rubber and used motor oil. *Int. J. Recent Technol. Eng, 8*(4), pp. 5501-5508, DOI: https://doi.org/10.35940/ijrte.D8893.118419

Deef-Allah, E. & Abdelrahman, M. (2021). Investigating the relationship between the fatigue cracking resistance and thermal characteristics of asphalt binders extracted from field mixes containing recycled materials. *Transportation Engineering, 4*, 100055. DOI: https://doi.org/10.1016/j.treng.2021.100055

Gao, L., Aguiar-Moya, J. P. & Zhang, Z. (2012). A Bayesian analysis of heterogeneity in modeling of pavement fatigue cracking. *Journal of Computing in Civil Engineering, 26*(1), pp. 37-43. DOI: http://dx.doi.org/10.1061/(ASCE)CP.1943-5487.0000114

Gibson, N., Seo, Y., Li, X., Adriescu, A. & Youtcheff, J. (2014). Full-scale and laboratory fatigue cracking performance of combined high-recycle and warm mix asphalt pavements. *2014 FAA Worldwide Airport Technology Transfer Conference*. Galloway, New Jersey, USA.

Grilli, A., Graziani, A., Bocci, E. & Bocci, M. (2016). Volumetric properties and influence of water content on the compactability of cold recycled mixtures. *Mater. Struct, 49*, pp. 4349-4362. DOI: https://doi.org/10.1617/s11527-016-0792-x

Huang, Y. H. (2004). *Pavement analysis and design*. 2nd ed. Prentice Hall, Inc: Upper Saddle River, New Jersey.

Hunter, R. N. (2017). Disproving bottom-up fatigue cracking in well-constructed asphalt pavements. *Proceedings of the Institution of Civil Engineers Construction Materials, 170*, CM4, pp. 178-185. DOI: http://dx.doi.org/10.1680/jcoma.16.00019

Indonesia Investments. (2021). Coal (Internet). Cited 2021 Dec 20. Available from: https://www.indonesia-investments.com/business/commodities/coal/item236

Jaskula, P. (2014). Influence of compaction effectiveness on interlayer bonding of asphalt layers. *The 9th International Conference. Environmental Engineering*. May, 2014.

Kim, H., Arraigada, M., Raab, C. & Partl, M. N. (2011). Numerical and experimental analysis for the interlayer behavior of double-layered asphalt pavement specimens. *Journal of Materials in Civil Engineering, 23*(1), pp. 12-20. DOI: https://doi.org/10.1061/(ASCE)MT.1943-5533.0000003

Lee, S. H., Vo, H. V. & Park, D. W. (2018). Investigation of asphalt track behavior under cyclic loading: full-scale testing and numerical simulation. *Journal of Testing and Evaluation, 46*(3), pp. 934-942. DOI: https://doi.org/10.1520/JTE20160554

Mackiewicz, P. (2018). Fatigue cracking in road pavement. *IOP Conf. Series: Materials Science and Engineering, 356*, 012014. DOI: https://doi.org/10.1088/1757-899X/356/1/012014

McGennis, R. B., Anderson, R. M., Kennedy, T. W. & Solaimanian M. (1994). Background of Superpave asphalt *mixture design and analysis*. Publication No. FHWA-SA-95-003.

Mensching, D. J., Rahbar-Rastegar, R., Underwood, B. S. & Daniel, J. S. (2016). Identifying indicators for fatigue cracking in hot-mix asphalt pavements using viscoelastic continuum damage principles. *Transportation Research Record: Journal of the Transportation Research Board, 2576*, pp. 28-39. DOI: http://dx.doi.org/10.3141/2576-04

Mohammad, L., Bae, A., Elseifi, M., Button, J. & Patel, N. (2010). Effects of pavement surface type and sample preparation method on tack coat interface shear strength. *Transportation Research Record: Journal of the Transportation Research Board, 2180*(1), pp. 93-101. DOI: https://doi.org/10.3141/2180-11

Mulungye, R. M., Owende, P. M. & Mellon, K. (2007). Finite element modelling of flexible pavements on soft soil subgrades. *Mater Des, 28*(3), pp. 739-756. DOI: https://doi.org/10.1016/j.matdes.2005.12.006

Nagy, A. A., El-Maaty, A. E. A. & Hashim, I. H. (2023). Evaluation of maintenance and rehabilitation treatments on long-term asphalt pavement performance. *Engineering Research Journal, 46*(1), pp. 65-81.

Powell, W. D., Potter, J. F., Mayhew, H. C. & Nunn, M. E. (1984). *The structural design of bituminous roads*. Transport & Road Research Laboratory: Crowthorne, UK, Report 1132.

Rahbar-Rastegar, R. (2017). Cracking in Asphalt Pavements: Impact of Component Properties and Aging on Fatigue and Thermal Cracking. University of New Hampshire: Ph.D. Thesis.

Rakyat Sulsel. (2022). Pemkot atur tonase dan kecepatan truk batubara di pare-pare (Internet). Cited 2022 Dec 16. Available from: https://rakyatsulsel.fajar.co.id/2022/03/24/pemkot-atur-tonase-dan-kecepatan-truk-batubara-di-parepare/

Roberts, F., Kandhal, P., Brown, E., Lee, D. & Kennedy, T. (1996). *Hot Mix Asphalt Materials Mixture Design and Construction*. 2nd ed: NAPA Education Foundation 603.

Saad, I., Sarsam, I. & Lutfi, A. Z. (2015). Resistance to moisture damage of recycled asphalt concrete pavement. *Journal of Engineering, 21*, pp. 45-54.

Setiawan, D. M. (2020). Structural response and sensitivity analysis of granular and asphaltic overlayment track considering linear viscoelastic behavior of asphalt. *Journal of the Mechanical Behavior of Materials, 29*, pp. 94-105. DOI: https://doi.org/10.1515/jmbm-2020-0010

Setiawan, D. M. (2021). Structural response and sensitivity analysis of granular and asphaltic overlayment track considering linear viscoelastic behavior of asphalt. *Journal of the Mechanical Behavior of Materials, 30*, pp. 66-86. DOI: https://doi.org/10.1515/jmbm-2021-0008

Setiawan, D. M. (2022a). Evaluation of Indonesia's conventional track performance based on mechanistic approach. *International Journal of Sustainable Construction Engineering and Technology, 13*(1), pp. 185-201. DOI: https://doi.org/10.30880/ijscet.2022.13.01.017

Setiawan, D. M. (2022b). Sub-grade service life and construction cost of ballasted, asphaltic underlayment, and combination rail track design. *Jordan Journal of Civil Engineering, 16*(1), pp. 173-192.

Setiawan, D. M. (2022c). Stress-strain characteristics and service life of conventional and asphaltic underlayment track under heavy load Babaranjang trains traffic. *Journal of the Mechanical Behavior of Materials, 31*, pp. 21-36. DOI: https://doi.org/10.1515/jmbm-2022-0003

Sulistyorini, R. (2015). Potensi kereta api sebagai angkutan barang di provinsi Lampung. *Jurnal Kelitbangan Provinsi,3*(2), pp. 1-15. (In Bahasa Indonesia).

Tschegg, E. K., Kroyer, G., Tan, D. M., Stanzl-Tschegg, S. E. & Litzka, J. (1995). Investigation of bonding between asphalt layers on road construction. *J. Transp. Eng, 121*(4), pp. 309-316.

Wang, H. & Al-Qadi, I. L. (2010). Near-surface pavement failure under multiaxial stress state in thick asphalt pavement. *Transportation Research Record: Journal of the Transportation Research Board, 2154*(1), pp. 91-99. DOI: https://doi.org/10.3141/2154-08

Xia, Y., Lin, J., Chen, Z., Cai, J., Hong, J. & Zhu, X. (2022). Fatigue cracking evolution and model of cold recycled asphalt mixtures during different curing times. *Materials, 15*, pp. 44-76. DOI: https://doi.org/10.3390/ma15134476

Yang, S. L., Baek, C. & Park, H. B. (2021). Effect of aging and moisture damage on fatigue cracking properties in asphalt mixtures. *Applied Sciences, 11*, 10543. DOI: https://doi.org/10.3390/app112210543